Engineered Porous Carbon for High Volumetric Methane Storage

J. Romanos[1,2,*], S. Sweany[1], T. Rash[1], L. Firlej[1,3], B. Kuchta[1,4], J.C. Idrobo[5] and P. Pfeifer[1] *(1) Department of Physics and Astronomy, University of Missouri, Columbia, MO 65211, USA. (2) Department of Natural Sciences, Lebanese American University, Byblos, Lebanon. (3) LCVN, Université Montpellier 2, 34095 Montpellier Cedex 5, France. (4) Laboratoire MARIDEL, Aix-Marseille Université, 13396 Marseille, France. (5) Advanced Microscopy Laboratory, Oak Ridge National Lab, Oak Ridge, TN 37831, USA.*

(Received date: 29 June 2014; Accepted date: 30 August 2014)

ABSTRACT: This paper covers the optimization of methane volumetric storage capacity by controlling the sub-nanometre (<1 nm) and supra-nanometre (1–5 nm) pore volumes. Nanospace engineering of KOH activated carbon generates an ideal structure for methane storage in which gas molecules are adsorbed as a high-density fluid by strong van der Waals forces into pores that are a few molecules in diameter. High specific surface areas, porosities, sub-nanometre (<1 nm) and supra-nanometre (1–5 nm) pore volumes are quantitatively selected by controlling the degree of carbon consumption and metallic potassium intercalation into the carbon lattice during the activation process. The formation of tuneable sub-nanometre and supra-nanometre pores is validated by sub-critical nitrogen adsorption. Aberration-corrected scanning transmission electron microscopy data show the atomic structure of high-surface-area activated carbon (2600 m^2/g). While high surface area and high porosity are optimal for gravimetric methane storage, the results indicate that an exclusive sub-nanometre region, a low porosity and an acceptable surface area (approximately 2000 m^2/g) are ideal for methane volumetric storage, storing 120 g CH_4/l (184 vol/vol) at 35 bar and room temperature (22 °C). High-pressure methane isotherms up to 150 bar at 30, –25 and –50 °C on optimal activated carbons are presented. Methane volumetric storage capacity at 35 bar reaches 176 g/l (269 vol/vol) and 202 g/l (309 vol/vol) at –25 and –50 °C, respectively.

1. INTRODUCTION

Natural gas (NG) provides 23% of the world's energy. NG reserves are increasing with new detection and extraction technologies. Hydraulic fracturing, which is currently used in the extraction of NG from shale rock formations, is having a dramatic impact on world's energy supply. According to the Energy Information Administration estimates, the United States possesses 2543 trillion cubic feet of technically recoverable NG. Methane hydrate reservoirs, found under sediments on the ocean floors, contain two to ten times the currently known reserves of NG. The high price of gasoline will allow NG to play an important role in shaping the energy industry in the years and decades to come. NG is a strong candidate for the auto and energy industry as a transitional solution before hydrogen and battery technologies mature.

In order to apply NG technology to vehicles, NG needs to be stored efficiently at high density. NG storage devices should provide an acceptable driving range of 482.8 km (300 mi) in a volume of space, which does not compromise a vehicle's volume and mass. The ability to refill and release large amounts of NG with sufficient flow rates from an obtrusive tank that operates within

*Author to whom all correspondence should be addressed. E-mail: jimmy.romanos@lau.edu.lb (J. Romanos).

acceptable pressure and temperature ranges is also required. All targets must be met at the end of service life of approximately 1500 cycles or 5000 operation hours or its equivalent of 2,41,401.6 km (1,50,000 mi). The targets are challenging, and extensive research and development efforts are being undertaken to achieve them. Compressed NG (CNG) and liquefied NG (LNG) are currently established technologies for the storage and transport of NG. The costs of compression and cooling, and heavy, expensive and non-conformable tanks limit the suitability of CNG and LNG for smaller vehicles. Adsorbed NG technology is an energy-efficient method for storing NG at room temperature and low pressure with applications that are not limited to the auto industry. The U.S. Department of Energy, under the ARPA-E Methane Opportunities for Vehicular Energy initiative, has set a methane volumetric target of 224 g/l in 2013, which is equivalent to 343 vol/vol.

Storage of NG in microporous materials was under development in the past (Bose *et al*. 1991; Mieville and Robinson 1998; Zhou *et al*. 2005; Ahmadpour *et al*. 2013, 2014). Activated carbon is a class of adsorbent materials with applications ranging from water treatment, gas and chemical purification, medical poisoning treatment to gas storage and sequestration (Matranga *et al*. 1992; Otowa *et al*. 1997; Bansal and Goyal 2005; Marsh and Rodríguez-Reinoso 2006; Gun'ko *et al*. 2011). As part of the Alliance for Collaborative Research in Alternative Fuel Technology, we have been working on optimizing activated carbon from corncob biomass feedstock for gas-storage applications for advanced transportation (Kuchta *et al*. 2010; Beckner *et al*. 2012; Kuchta *et al*. 2012; Romanos *et al*. 2012c; Romanos *et al*. 2013). Both physical and chemical activation of carbon samples have been widely investigated for several activation agents (Caturla *et al*. 1991; Rodríguez-Reinoso and Molina-Sabio 1992; Rodríguez-Reinoso *et al*. 1995; Romanos *et al*. 2012b). In this work, NG storage by physisorption on high-surface-area activated carbons is presented. Optimal pore structure resulting in higher methane uptake was studied in detail. In order to change the pore structure of activated carbon, one has to understand the activation mechanism and how the activation agent concentration and activation temperature affect the pore structure.

2. CONTROLLING THE PORE STRUCTURE OF ACTIVATED CARBON

Physical and chemical activation of carbon has been widely investigated for several activation agents (Caturla *et al*. 1991; Rodríguez-Reinoso and Molina-Sabio 1992; Rodríguez-Reinoso *et al*. 1995). KOH activated carbon is an effective gas adsorbent primarily due to its high porosity and large surface area. The search for high-performance NG adsorbents is carried out by numerous research groups worldwide. This search is a complex landscape of *structure–function* relationships—structure being physical and chemical characteristics of the adsorbing surface and surrounding pore space, function being volumetric and gravimetric storage capacity. In a previous study, we showed how to control the number of supra-nanometre pores in a manner not achieved previously by chemical activation (Romanos *et al*. 2012a). The chemical mechanism underlying this control was studied by following the evolution of elemental composition, specific surface area, porosity and pore-size distribution during KOH activation and preceding H_3PO_4 activation. The oxygen, nitrogen and hydrogen contents decrease during successive activation steps, creating a nanoporous carbon network with a porosity and surface area controllable for various applications (Romanos *et al*. 2012a). The same process can be used to synthesize an activated carbon structure optimal for volumetric storage capacity. High-resolution scanning transmission electron microscopy (STEM) in Figure 1 shows that activated carbon grains are formed of corrugated

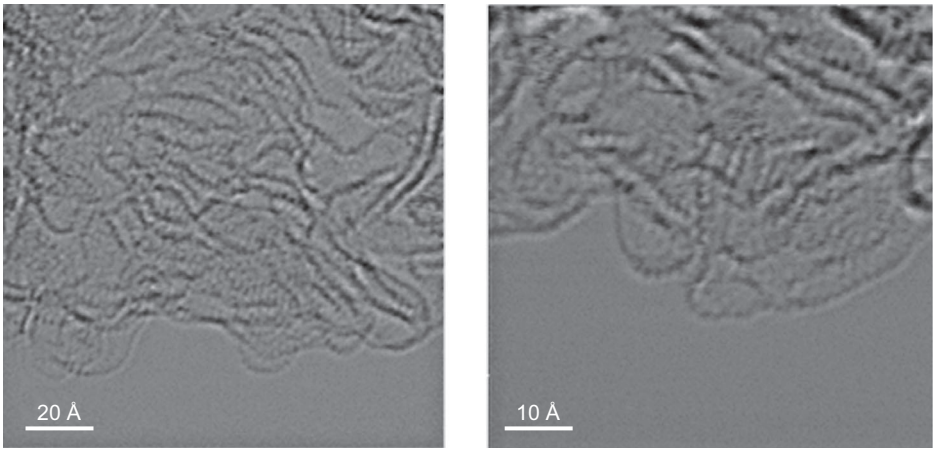

Figure 1. High-resolution STEM bright-field micrograph of high-surface-area activated carbon (2600 m^2/g).

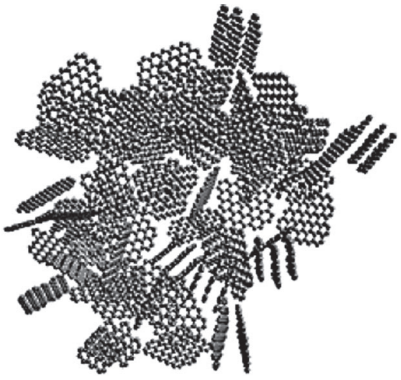

Figure 2. Model of an activated carbon grain.

carbon sheets (Figure 2) with typical dimensions of 2–5 nm. The absence of graphitic components, visible in low-surface area carbon, indicates that the carbon has been completely activated. The activation degree is controlled by increasing the activation agent concentration (KOH:C weight ratio) at an activation temperature of 700 °C. Methane is a spherical molecule; it is adsorbed by strong van der Waals forces in pores of few molecular diameters as a high-density fluid. Figure 3 shows a slit-shaped pore. Figures 4 and 5 are a simple representation of the effect of pore structure on methane adsorption. This simple representation is based on methane–carbon interactions in infinite slit-shaped micropores by Steele's 10–4 potential function (Steele 1974; Gusev *et al*. 1997).

$$\phi_{C-CH_4}(z) = A\left[\frac{2}{5}\left(\frac{\sigma_{C-CH_4}}{z}\right)^{10} - \left(\frac{\sigma_{C-CH_4}}{z}\right)^{4}\right] \tag{1}$$

where A = 16.69 kJ/mol (2008 K) and $\sigma_{C\text{-}Ch4}$ = 3.61 Å (Tan and Gubbins 1990) is the zero of the potential. The total potential is the sum of the potentials overlapping from each wall of the slit-shaped pore of width H.

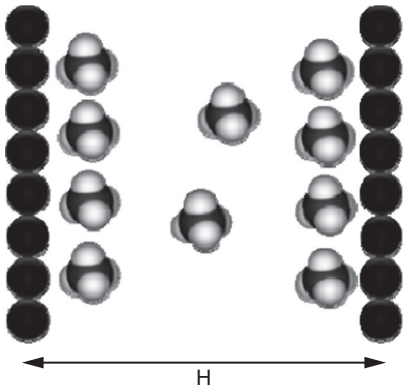

Figure 3. Slit-shaped pore.

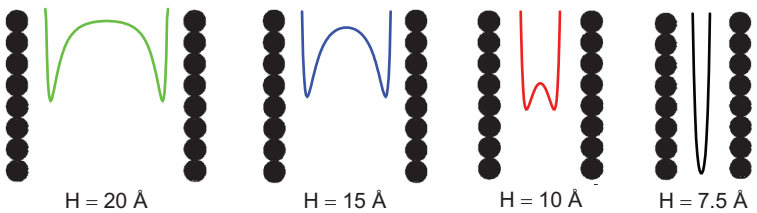

Figure 4. Adsorption potential for different pore widths.

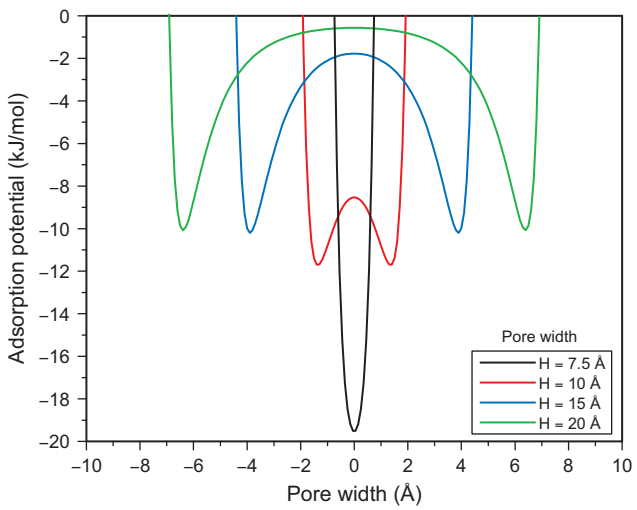

Figure 5. Adsorption potential for different pore widths (graphical).

$$\Phi_{\text{total}}(z) = \phi(z) + \phi(H - z) \tag{2}$$

For smaller pores, the potentials from opposite sides of the wall overlap. Consequently, the storage density (g CH_4/l carbon) of methane will be higher. However, the mass of the carbon increases and the gravimetric storage capacity (g CH_4/kg carbon) decreases. For larger

pores, the opposite situation occurs with a lower volumetric storage density and a higher gravimetric storage capacity. In this work, we will demonstrate how to control the sub-nanometre and supra-nanometre pore volumes and the effect of the pore structure on methane storage.

3. EXPERIMENTAL METHODS

3.1. Sample Preparation and Sub-Critical Nitrogen Adsorption

Activated carbon samples were prepared in a multi-step activation process from corncob biomass waste feedstock. During phosphoric acid activation, corncob was soaked in phosphoric acid for 12 hours in an oven at 45 °C. The mixture was then charred at 480 °C in a nitrogen environment. Charred carbon was then washed with hot water until it neutralizes (pH = 7). Activation of the resulting carbon with KOH flakes was performed at a selected temperature and KOH concentration for 1 hour. The resulting material is washed with water (pH = 7) and dried to form the final product.

Sub-critical nitrogen isotherms at 77 K were performed on a QUADRASORB surface analyzer (Quantachrome Instruments, Boynton Beach, FL), which was periodically calibrated using a surface area reference material SARM 2012 (768 m^2/g) provided by Quantachrome. Specific surface areas ($\sum$) are determined from sub-critical nitrogen isotherms using the BET theory in the pressure range of 0.01–0.03 P/P_0, which is suitable for microporous materials. Surface areas larger than 1000 m^2/g were rounded to the nearest hundred. The total pore volume (V_{tot}) is determined at a pressure of 0.995 P/P_0. The porosity ϕ, defined as the volume fraction occupied by open pores, is calculated as follows:

$$\phi = \left[1 + \left(\rho_{skel} \times \frac{V_{tot}}{m_s}\right)^{-1}\right]^{-1} \tag{3}$$

$$\rho_{app} = \rho_{skel}\left(1 - \phi\right) \tag{4}$$

where ρ_{skel} is the skeletal density of the sample, assumed to be 2.0 g/cm^3. Typical skeletal densities of amorphous carbons are between 1.8 and 2.1 g/cm^3 (Lide 2005). The apparent density (ρ_{app}), which can be calculated from equation (2), is the density of the material taking into consideration the volume of open pores and the skeletal volume of carbon.

Quenched solid-density functional theory (QSDFT) for infinite slit-shaped pores is used for calculating the pore-size distribution. QSDFT is a modified version of the non-local density functional theory (NLDFT). NLDFT, which assumes a flat graphitic pore structure, has a significant drawback when applied to activated carbons where heterogeneities obstruct layering transitions, thus leading to false minimums in the pore-size distribution. This artefact has been completely eliminated with QSDFT by considering surface roughness and heterogeneity. The surface is modelled using the distribution of solid atoms rather than the source of the external potential field (Ravikovitch and Neimark 2006; Neimark *et al*. 2009). As a consequence, the resulting QSDFT pore-size distributions are more reliable for nanoporous activated carbon.

3.2. Scanning Transmission Electron Microscopy

Samples were prepared for STEM by dispersing the carbon in methanol and depositing it on holey carbon support films (Harris *et al*. 2008). STEM micrographs in Figure 1 were taken at the Advanced Microscopy Laboratory at Oak Ridge National Laboratory using Nion UltraSTEM 100 STEM with a third-generation C3/C5 aberration corrector. This instrument is capable of atomic resolution imaging at mid and low voltages with single atom sensitivity; 60 keV was used in order to avoid beam damage.

3.3. Excess Adsorption

Gravimetric excess adsorption is the mass of the adsorbed film minus the mass of an equal volume of gas. Dry sample mass was determined by measuring the sample mass under vacuum after heating it to 400 °C for 2 hours under vacuum (2.7 kPa).

3.3.1. Gravimetric Methane Measurements

A gravimetric measurement of excess adsorption at 35 bar and 22 °C on activated carbons is made by taking the following four mass measurements: mass of evacuated sample cell (m_C), mass of cell and methane gas ($m_{C,G}$), mass of cell and outgassed sample ($m_{C,S}$) and mass of cell with sample and gas ($m_{C,S,G}$). This simple and unique method developed at the University of Missouri requires no relevant buoyancy-related corrections. The excess mass adsorption by mass sample per sample mass is as follows:

$$\frac{m^e}{m_{sample}} = \frac{m_{C,S,G} - m_{C,G}}{m_{C,S} - m_C} - 1 - \frac{\rho_{gas}}{\rho_{skel}} \tag{5}$$

where ρ_{skel} is the skeletal density of activated carbon: $\rho_{skel} = 2$ g/cm^3. ρ_{gas} is the density of the gas at the corresponding pressure from the National Institute of Standards and Technology Reference Fluid Thermodynamic and Transport Properties Database.

3.3.2. Volumetric Methane Measurements

Methane adsorption isotherms were measured volumetrically using an HTP-1 volumetric adsorption analyzer (Hiden Isochema Ltd., Warrington, UK). Methane measurements were performed at temperatures of 30, –25 and –50 °C at pressures ranging from 1 to 150 bar.

3.4. Gravimetric and Volumetric Storage Capacity

The total gravimetric storage capacity per sample mass (g/kg) is determined from the excess adsorption using the porosity ϕ of the sample determined from nitrogen isotherms.

$$\frac{m^{stored}}{m_{sample}} = \frac{m^e}{m_{sample}} + \frac{\rho_{gas}}{\rho_{skel}}\left(\frac{\phi}{1-\phi}\right) \tag{6}$$

The volumetric storage capacity is obtained by multiplying the gravimetric storage capacity with the apparent density, which is calculated using $\rho_{app} = \rho_{skel}(1 - \phi)$

$$\frac{m^{stored}}{V_{sample}} = \frac{m^{stored}}{m_{sample}} \times \rho_{app} \tag{7}$$

The porosity measured by sub-critical nitrogen adsorption represents the intragranular porosity. Consequently, the gravimetric and volumetric storage capacities in this paper represent activated carbon particle performance and not the complete system performance because the void between particles is not taken into account by this method.

4. RESULTS AND DISCUSSIONS

To control the pore structure, the activation agent (KOH) concentration is varied and its effects on porosity, BET surface area and pore-size distribution are measured. Figure 6 shows the effect of increasing the activation agent concentration (KOH:C weight ratios of 2, 2.5, 3, 3.5, 4 and 4.5) for a constant activation temperature of 700 °C. The number of sub-nanometre pores (<1 nm) shows a moderate decrease by increasing the KOH:C weight ratio, whereas the number of supra-nanometre pores (1–5 nm) increases by increasing the KOH:C weight ratio. In addition, the cumulative pore volume, which is related to the porosity, increases by increasing the KOH:C weight ratio. Samples activated at 700 °C and having a KOH:C weight ratio below 2.5 have an almost exclusive sub-nanometre pore structure. The pores fraction as a function of activation agent concentration is presented in Figure 7. The supra-nanometre pore volume is proportional to the KOH:C weight ratio. In fact, by increasing the KOH:C weight ratio, the number of metallic potassium penetrating into the carbon matrix increases. Consequently, the carbon matrix will be enlarged, and larger pores will be created. In addition, the amount of supra-nanometre pore volumes can be controlled by selecting appropriate KOH:C weight ratio, which leads to the possibility of optimal pore-size selection for methane storage. It is important to note that for a

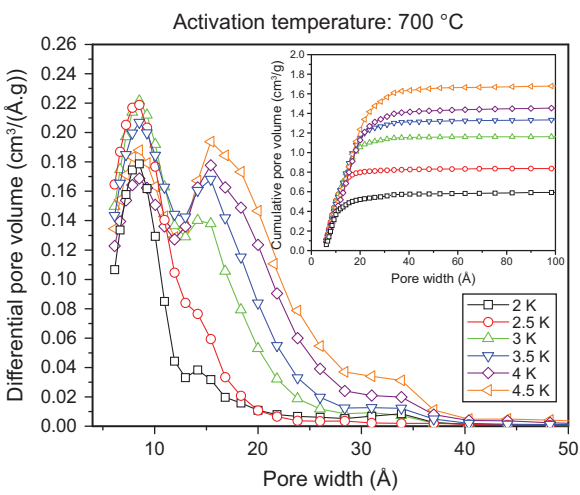

Figure 6. Effect of KOH:C weight ratio and the activation temperature on the pore-size distribution. The inset shows the cumulative pore volume.

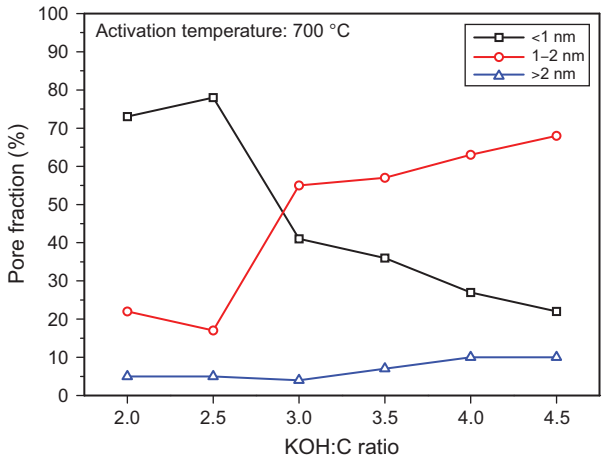

Figure 7. Pore fraction as a function of the activation agent concentration.

KOH:C weight ratio equal to 2.5 and 3, the largest sub-nanometre pore volume occurs. In fact, a fraction of sub-pores will be transformed to supra-nanometre pores with higher KOH:C weight ratio. Moreover, for a KOH:C weight ratio equal to 2.5, we have also a small supra-nanometre pore volume.

Several parameters should be considered during the optimization process. The first is methane binding energy, which is higher in sub-nanometre (<1 nm) pores than in supra-nanometre (1–5 nm) pores because of the overlapping potential. Consequently, the optimal sample requires a large sub-nanometre (<1 nm) pore volume. The second is the specific surface area. A high specific surface area increases the methane excess adsorption; this relation is known as Chahine's rule (Sevilla *et al*. 2010). The third is the total porosity, which is defined as the volume fraction occupied by open pores. The volumetric storage capacity increases by increasing excess adsorption and decreasing material porosity. However, the gravimetric storage capacity increases by increasing both. Figure 8 shows that the methane excess adsorption and the gravimetric storage capacity are proportional to the KOH:C weight ratio. This means that samples with large supra-nanometre region are more suited for gravimetric storage capacity. By contrast, samples with an exclusive sub-nanometre region are more suited for volumetric storage capacity. For a KOH:C weight ratio equal to 2, the activation process generates a low porosity (0.58) and a low surface area (1300 m^2/g). Despite the low porosity, the volumetric storage capacity is low because of the low surface area. For a KOH:C weight ratio equal to 2.5, the surface area increases to 2000 m^2/g and the porosity to 0.66. This particular combination of an acceptable high surface area and low porosity generates a high volumetric storage capacity. Sample 2.5K activated at 700 °C meets these conditions, and has a volumetric storage capacity of 120 g/l. This particular combination of low porosity and acceptable surface area can be achieved at a higher activation temperature and a lower activation agent concentration. Figures 9 and 10 show the excess adsorption and the gravimetric storage capacity of the optimal sample at 30, –25 and –50 °C up to 150 bar. Figure 11 shows the volumetric storage capacity of the optimal sample at 30, –25 and –50 °C up to 150 bar. Methane volumetric storage capacity at 35 bar reaches 176 and 202 g/l at –25 and –50 °C, respectively. For larger KOH:C weight ratios, both the specific surface area and the porosity

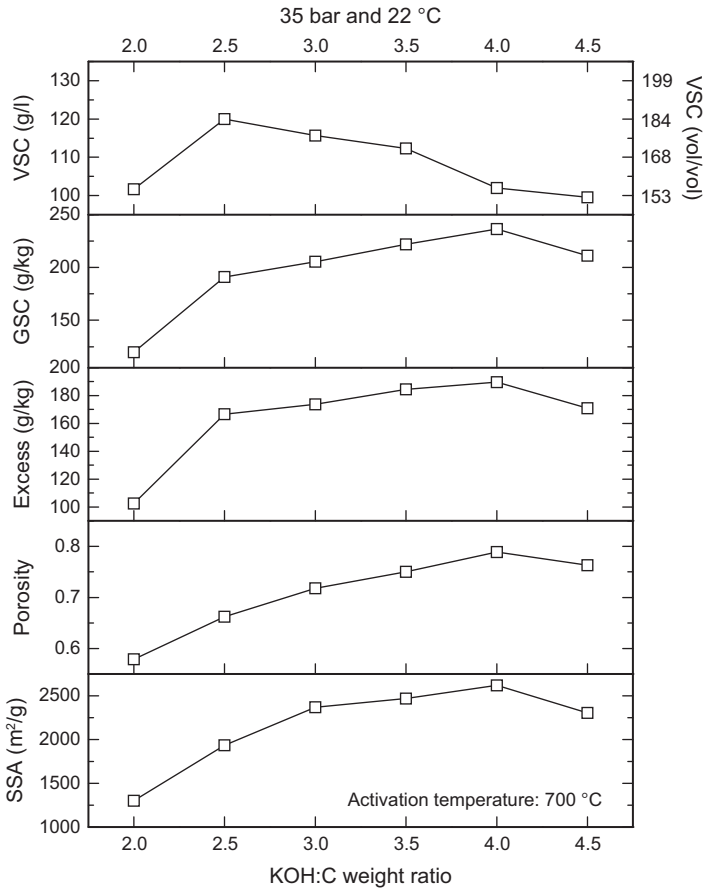

Figure 8. Specific surface area (SSA), porosity, methane excess adsorption (gravimetric method), gravimetric storage capacity (GSC) and volumetric storage capacity (VSC) as a function of KOH:C weight ratio.

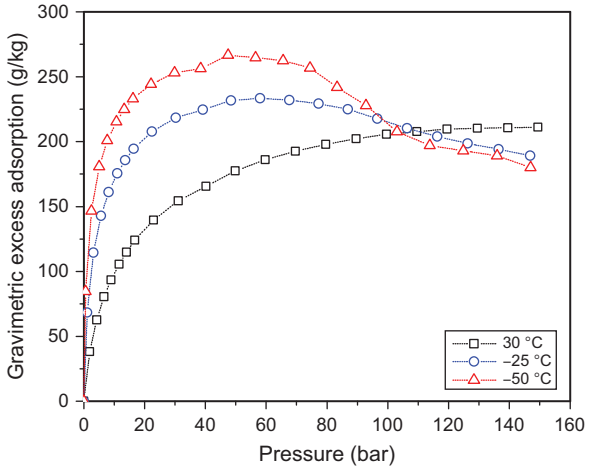

Figure 9. Excess adsorption of the optimal sample (measured by the volumetric method on HTP-1; Hiden Isochema Ltd., Warrington, UK) at 30, –25 and –50 °C.

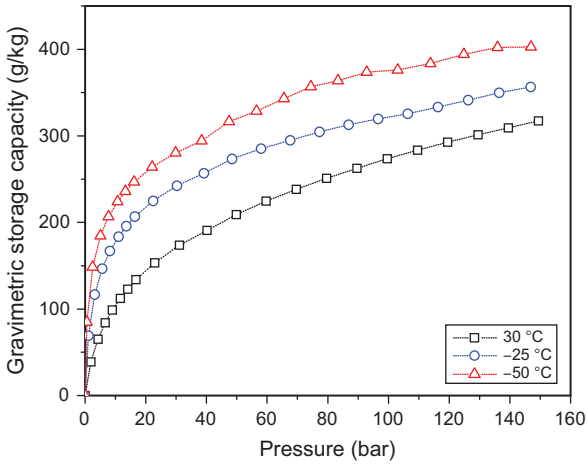

Figure 10. Gravimetric storage capacity of the optimal sample at 30, –25 and –50 °C.

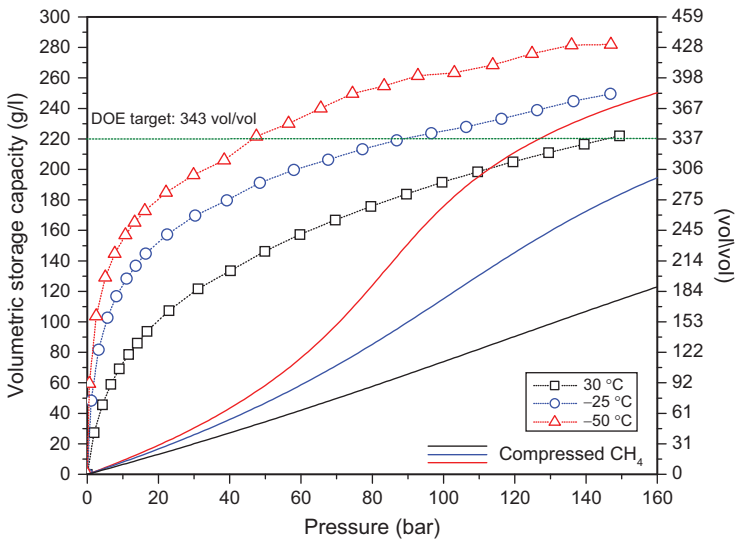

Figure 11. Volumetric storage capacity of the optimal sample at 30, –25 and –50 °C. DOE = Department of Energy.

increase up to 2500 m^2/g and 0.78. respectively, resulting in higher excess adsorption; however, volumetric storage capacity decreases because of the increase in porosity.

5. CONCLUSION

A combination of an acceptable high surface area and low porosity generates a high methane volumetric storage capacity. In this work, this combination is achieved by selecting appropriate activation agent concentration and activation temperature. The performance of this sample is 120 g CH_4 per litre carbon at 35 bar and room temperature.

ACKNOWLEDGEMENTS

This research is based on the work supported by the California Energy Commission under Contract No. 500-08-022. STEM experiments were conducted at the Center for Nanophase Materials Sciences, which is sponsored at Oak Ridge National Laboratory by the Scientific User Facilities Division, Office of Basic Energy Sciences, U.S. Department of Energy.

REFERENCES

Ahmadpour, A., Jahanshahi, N., Rashidi, S., Chenarani N. and Mahboub, M.J.D. (2014) *Adsorpt. Sci. Technol.* **32**, 275.

Ahmadpour, A., Rashidi, H., Mahboub, M.J.D. and Farmad, M.R. (2013) *Adsorpt. Sci. Technol.* **31**, 729.

Bansal, R.C. and Goyal M. (2005) *Activated Carbon Adsorption*, Taylor & Francis, Boca Raton, FL.

Beckner, M., Romanos, J., Dohnke, E., Singh, A., Schaeperkoetter, J., Stalla, D., Burress, J., Jalisatgi, S., Suppes, G. and Hawthorne, M. (2012) *Bull. Am. Phys. Soc.* **57**, 33007.

Bose, T.K., Chahine, R. and St-Arnaud, J.-M. (1991) "High-density adsorbent and method of producing same." *U.S. Patent No. 4.499.330.*

Caturla, F., Molina-Sabio, M. and Rodríguez-Reinoso, F. (1991) *Carbon.* **29**, 999.

Gun'ko, V., Turov, V., Kozynchenko, O., Nikolaev, V., Tennison, S., Meikle, S., Snezhkova, E., Sidorenko, A., Ehrburger-Dolle, F., Morfin, I., Klymchuk, D. and Mikhalovsky, S. (2011) *Adsorption.* **17**, 453.

Gusev, V.Y., O'Brien, J.A. and Seaton, N.A. (1997) *Langmuir.* **13**, 2815.

Harris, P.J., Liu, Z. and Suenaga, K. (2008) *J. Phys.: Condens. Matter.* **20**, 362201.

Kuchta, B., Firlej, L., Mohammadhosseini, A., Beckner, M., Romanos, J. and Pfeifer, P. (2012a) *J. Mol. Model.* **19**, 4079.

Kuchta, B., Firlej, L., Mohammadhosseini, A., Boulet, P., Beckner, M.W., Romanos, J. and Pfeifer, P. (2012b) *J. Am. Chem. Soc.* **134**, 15130.

Kuchta, B., Firlej, L., Roszak, S. and Pfeifer, P. (2010) *Adsorption.* **16**, 413.

Lide, D.R. (2005) *CRC Handbook of Chemistry and Physics* (CD-ROM), CRC Press, London, UK.

Marsh, H. and Rodríguez-Reinoso, F. (2006) *Activated Carbon*, Elsevier, Amsterdam, Netherlands/London, UK.

Matranga, K.R., Myers, A.L. and Glandt, E.D. (1992) *Chem. Eng. Sci.* **47**, 1569.

Mieville, R.L. and Robinson, K.K. (1998) "Monolithic carbonaceous article." *US Patent App. 08/600*, 882.

Neimark, A.V., Lin, Y., Ravikovitch, P.I. and Thommes, M. (2009) *Carbon.* **47**, 1617.

Otowa, T., Nojima, Y. and Miyazaki, T. (1997) *Carbon.* **35**, 1315.

Ravikovitch, P.I. and Neimark, A.V. (2006) *Langmuir.* **22**, 11171.

Rodríguez-Reinoso, F. and Molina-Sabio, M. (1992) *Carbon.* **30**, 1111.

Rodríguez-Reinoso, F., Molina-Sabio, M. and González, M.T. (1995) *Carbon.* **33**, 15.

Romanos, J., Beckner, M., Rash, T., Firlej, L., Kuchta, B., Yu, P., Suppes, G., Wexler, C. and Pfeifer, P. (2012b) *Nanotechnology.* **23**, 015401.

Romanos, J., Beckner, M., Rash, T., Yu, P., Suppes, G. and Pfeifer, P. (2012c) *Bull. Am. Phys. Soc.* **54,** 27009.

Romanos, J., Burress, J., Pfeifer, P., Rash, T., Shah, P. and Suppes, G. (2012a) "High surface area carbon and process for its production." *U.S. Patent App. 13/717*, 388.

Romanos, J., Beckner, M., Stalla, D., Tekeei, A., Suppes, G., Jalisatgi, S., Lee, M., Hawthorne, F., Robertson, J.D., Firlej, L., Kuchta, B., Wexler, C., Yu, P. and Pfeifer, P. (2013) *Carbon.* **54**, 208.

Sevilla, M., Alam, N. and Mokaya, R. (2010) *J. Phys. Chem. C.* **114**, 11314.

Steele, W.A. (1974) *The Interaction of Gases with Solid Surfaces*, Oxford, UK/New York, Pergamon Press.

Tan, Z. and Gubbins, K.E. (1990) *J. Phys. Chem.* **94**, 6061.

Zhou, Y., Wang, Y., Chen, H. and Zhou, L. (2005) *Carbon.* **43**, 2007.